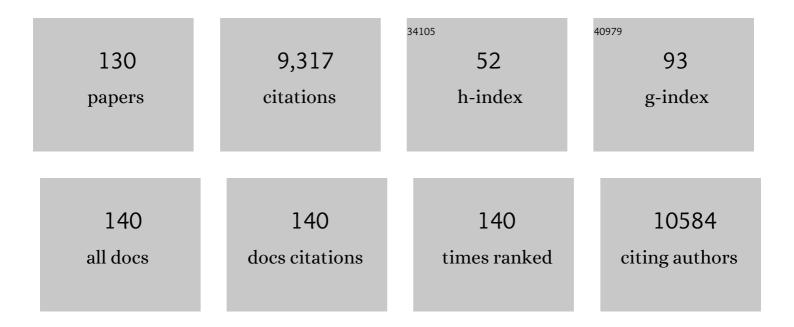


## List of Publications by Year in descending order

Source: https://exaly.com/author-pdf/6501951/publications.pdf Version: 2024-02-01



<u> \λ/ει Ελ</u>δ

#	Article	IF	CITATIONS
1	Titrating Controlled Defects into Si-LTA Zeolite Crystals Using Multiple Organic Structure-Directing Agents. Chemistry of Materials, 2022, 34, 1789-1799.	6.7	6
2	P-Site Structural Diversity and Evolution in a Zeosil Catalyst. Journal of the American Chemical Society, 2021, 143, 1968-1983.	13.7	17
3	Exfoliation of surfactant swollen layered MWW zeolites into two-dimensional zeolite nanosheets using telechelic liquid polybutadiene. Microporous and Mesoporous Materials, 2021, 315, 110883.	4.4	10
4	Innentitelbild: Enabling Lithium Metal Anode in Nonflammable Phosphate Electrolyte with Electrochemically Induced Chemical Reactions (Angew. Chem. 35/2021). Angewandte Chemie, 2021, 133, 19042-19042.	2.0	0
5	Enabling Lithium Metal Anode in Nonflammable Phosphate Electrolyte with Electrochemically Induced Chemical Reactions. Angewandte Chemie - International Edition, 2021, 60, 19183-19190.	13.8	36
6	Enabling Lithium Metal Anode in Nonflammable Phosphate Electrolyte with Electrochemically Induced Chemical Reactions. Angewandte Chemie, 2021, 133, 19332-19339.	2.0	1
7	Adsorption-Enhanced Glucan Oligomer Production from Cellulose Hydrolysis over Hyper-Cross-Linked Polymer in Molten Salt Hydrate. ACS Applied Materials & Interfaces, 2021, 13, 52082-52091.	8.0	12
8	Identifying Order and Disorder in Double Four-Membered Rings via Raman Spectroscopy during Crystallization of LTA Zeolite. Chemistry of Materials, 2021, 33, 6794-6803.	6.7	8
9	Beyond biodegradation: Chemical upcycling of poly(lactic acid) plastic waste to methyl lactate catalyzed by quaternary ammonium fluoride. Journal of Catalysis, 2021, 402, 61-71.	6.2	12
10	Separation of short-chain glucan oligomers from molten salt hydrate and hydrolysis to glucose. Green Chemistry, 2021, 23, 4114-4124.	9.0	15
11	Monte carlo simulations and experiments of all-silica zeolite LTA assembly combining structure directing agents that match cage sizes. Physical Chemistry Chemical Physics, 2021, 24, 142-148.	2.8	1
12	A stable aluminosilicate zeolite with intersecting three-dimensional extra-large pores. Science, 2021, 374, 1605-1608.	12.6	59
13	Role of Silica Support in Phosphoric Acid Catalyzed Production of <i>p</i> -Xylene from 2,5-Dimethylfuran and Ethylene. Industrial & Engineering Chemistry Research, 2020, 59, 22049-22056.	3.7	14
14	Bimodal Mesoporous Carbon Spheres with Small and Ultra-Large Pores Fabricated Using Amphiphilic Brush Block Copolymer Micelle Templates. ACS Applied Materials & Interfaces, 2020, 12, 57322-57329.	8.0	22
15	One-Step Synthesis of Hierarchical, Bimodal Nanoporous Carbons via Co-templating with Bottlebrush and Linear Block Copolymers. Chemistry of Materials, 2020, 32, 6055-6061.	6.7	16
16	The essential mass transfer step in hierarchical/nano zeolite: surface diffusion. National Science Review, 2020, 7, 1630-1632.	9.5	28
17	One-pot hydrodeoxygenation of biomass furan derivatives into decane under mild conditions over Pd/C combined with phosphotungstic acid. Green Chemistry, 2020, 22, 2889-2900.	9.0	27
18	Production of high-yield short-chain oligomers from cellulose <i>via</i> selective hydrolysis in molten salt hydrates and separation. Green Chemistry, 2019, 21, 5030-5038.	9.0	32

#	Article	IF	CITATIONS
19	Stable Multimetallic Nanoparticles for Oxygen Electrocatalysis. Nano Letters, 2019, 19, 5149-5158.	9.1	94
20	Adsorptive Nature of Surface Barriers in MFI Nanocrystals. Langmuir, 2019, 35, 12407-12417.	3.5	12
21	Selective Production of Aromatics by Catalytic Fast Pyrolysis of Furan with In Situ Dehydrogenation of Propane. ACS Catalysis, 2019, 9, 2626-2632.	11.2	25
22	Critical Role of Tricyclic Bridges Including Neighboring Rings for Understanding Raman Spectra of Zeolites. Journal of the American Chemical Society, 2019, 141, 20318-20324.	13.7	32
23	Fabrication of hierarchical Lewis acid Sn-BEA with tunable hydrophobicity for cellulosic sugar isomerization. Microporous and Mesoporous Materials, 2019, 278, 387-396.	4.4	30
24	Production of liquid fuel intermediates from furfural via aldol condensation over potassium-promoted Sn-MFI catalyst. Fuel, 2019, 237, 1281-1290.	6.4	33
25	Broadening the Scope for Fluorideâ€Free Synthesis of Siliceous Zeolites. Angewandte Chemie - International Edition, 2018, 57, 3607-3611.	13.8	56
26	Intraparticle Diffusional versus Site Effects on Reaction Pathways in Liquidâ€Phase Cross Aldol Reactions. ChemPhysChem, 2018, 19, 386-401.	2.1	5
27	Rücktitelbild: Broadening the Scope for Fluorideâ€Free Synthesis of Siliceous Zeolites (Angew. Chem.) Tj ETQq1	10.7843	314 rgBT /O
28	Silica Nanoparticle Mass Transfer Fins for MFI Composite Materials. Chemistry of Materials, 2018, 30, 2353-2361.	6.7	22
29	Tuning solid catalysts to control regioselectivity in cross aldol condensations with unsymmetrical ketones for biomass conversion. Molecular Catalysis, 2018, 458, 247-260.	2.0	12
30	Broadening the Scope for Fluorideâ€Free Synthesis of Siliceous Zeolites. Angewandte Chemie, 2018, 130, 3669-3673.	2.0	12
31	Renewable Isoprene by Sequential Hydrogenation of Itaconic Acid and Dehydra-Decyclization of 3-Methyl-Tetrahydrofuran. ACS Catalysis, 2017, 7, 1428-1431.	11.2	72
32	Tandem Diels–Alder Reaction of Dimethylfuran and Ethylene and Dehydration to <i>para</i> â€Xylene Catalyzed by Zeotypic Lewis Acids. ChemCatChem, 2017, 9, 2523-2535.	3.7	34
33	Exfoliation of two-dimensional zeolites in liquid polybutadienes. Chemical Communications, 2017, 53, 7011-7014.	4.1	29
34	Highly effective antibacterial activity by the synergistic effect of three dimensional ordered mesoporous carbon-lysozyme composite. Journal of Colloid and Interface Science, 2017, 503, 131-141.	9.4	19
35	The effects of ZSM-5 mesoporosity and morphology on the catalytic fast pyrolysis of furan. Green Chemistry, 2017, 19, 3549-3557.	9.0	72
36	Biomass-Derived Butadiene by Dehydra-Decyclization of Tetrahydrofuran. ACS Sustainable Chemistry and Engineering, 2017, 5, 3732-3736.	6.7	84

#	Article	IF	CITATIONS
37	Ultra-selective high-flux membranes from directly synthesized zeolite nanosheets. Nature, 2017, 543, 690-694.	27.8	446
38	A Review of Biorefinery Separations for Bioproduct Production via Thermocatalytic Processing. Annual Review of Chemical and Biomolecular Engineering, 2017, 8, 115-137.	6.8	24
39	The effects of contact time and coking on the catalytic fast pyrolysis of cellulose. Green Chemistry, 2017, 19, 286-297.	9.0	67
40	Spatially isolated palladium in porous organic polymers by direct knitting for versatile organic transformations. Journal of Catalysis, 2017, 355, 101-109.	6.2	40
41	Production of liquid fuel intermediates from furfural via aldol condensation over Lewis acid zeolite catalysts. Catalysis Science and Technology, 2017, 7, 3555-3561.	4.1	66
42	Free-standing porous carbon electrodes derived from wood for high-performance Li-O2 battery applications. Nano Research, 2017, 10, 4318-4326.	10.4	64
43	Oneâ€Pot Conversion of Carbohydrates into 5â€(Hydroxymethyl)furfural using Heterogeneous Lewisâ€Acid and BrÃ,nstedâ€Acid Catalysts. Energy Technology, 2017, 5, 747-755.	3.8	41
44	Renewable <i>p</i> â€Xylene from 2,5â€Dimethylfuran and Ethylene Using Phosphorusâ€Containing Zeolite Catalysts. ChemCatChem, 2017, 9, 398-402.	3.7	118
45	Effects of the Framework and Mesoporosity on the Catalytic Activity of Hierarchical Zeolite Catalysts in Benzyl Alcohol Conversion. ChemCatChem, 2016, 8, 2406-2414.	3.7	15
46	On the effectiveness of tailored mesoporous MFI zeolites for biomass catalytic fast pyrolysis. Applied Catalysis A: General, 2016, 522, 109-119.	4.3	106
47	Tuning the adsorption and separation properties of noble gases and N2 in CuBTC by ligand functionalization. RSC Advances, 2016, 6, 91093-91101.	3.6	11
48	Long Walks in Hierarchical Porous Materials due to Combined Surface and Configurational Diffusion. Chemistry of Materials, 2016, 28, 7852-7863.	6.7	53
49	Adsorption-enhanced hydrolysis of glucan oligomers into glucose over sulfonated three-dimensionally ordered mesoporous carbon catalysts. Green Chemistry, 2016, 18, 6637-6647.	9.0	25
50	Tunable Oleo-Furan Surfactants by Acylation of Renewable Furans. ACS Central Science, 2016, 2, 820-824.	11.3	64
51	Adsorption and reaction properties of SnBEA, ZrBEA and H-BEA for the formation of p-xylene from DMF and ethylene. Catalysis Science and Technology, 2016, 6, 5729-5736.	4.1	36
52	Antimicrobial Activity of Silver Ions Released from Zeolites Immobilized on Cellulose Nanofiber Mats. ACS Applied Materials & Interfaces, 2016, 8, 3032-3040.	8.0	99
53	An examination of alkali-exchanged BEA zeolites as possible Lewis-acid catalysts. Microporous and Mesoporous Materials, 2016, 225, 472-481.	4.4	23
54	Inhibition of Xylene Isomerization in the Production of Renewable Aromatic Chemicals from Biomass-Derived Furans. ACS Catalysis, 2016, 6, 2076-2088.	11.2	25

#	Article	IF	CITATIONS
55	Kinetic regimes in the tandem reactions of H-BEA catalyzed formation of p-xylene from dimethylfuran. Catalysis Science and Technology, 2016, 6, 178-187.	4.1	39
56	Dye-Sensitized Core/Active Shell Upconversion Nanoparticles for Optogenetics and Bioimaging Applications. ACS Nano, 2016, 10, 1060-1066.	14.6	395
57	Lewis acid zeolites for tandem Diels–Alder cycloaddition and dehydration of biomass-derived dimethylfuran and ethylene to renewable p-xylene. Green Chemistry, 2016, 18, 1368-1376.	9.0	140
58	Diels–Alder cycloaddition of 2-methylfuran and ethylene for renewable toluene. Applied Catalysis B: Environmental, 2016, 180, 487-496.	20.2	102
59	Reactive Liftoff of Crystalline Cellulose Particles. Scientific Reports, 2015, 5, 11238.	3.3	5
60	Quantitative carbon detector (QCD) for calibration-free, high-resolution characterization of complex mixtures. Lab on A Chip, 2015, 15, 440-447.	6.0	39
61	Three Dimensionally Ordered Mesoporous Carbon as a Stable, Highâ€Performance Li–O <sub>2</sub> Battery Cathode. Angewandte Chemie - International Edition, 2015, 54, 4299-4303.	13.8	175
62	Modelling the assembly of nanoporous silica materials. International Reviews in Physical Chemistry, 2015, 34, 35-70.	2.3	28
63	2D Surface Structures in Small Zeolite MFI Crystals. Chemistry of Materials, 2015, 27, 4650-4660.	6.7	37
64	Kinetic Regime Change in the Tandem Dehydrative Aromatization of Furan Diels–Alder Products. ACS Catalysis, 2015, 5, 2367-2375.	11.2	96
65	Fluoride-free synthesis of a Sn-BEA catalyst by dry gel conversion. Green Chemistry, 2015, 17, 2943-2951.	9.0	97
66	Effect of water treatment on Sn-BEA zeolite: Origin of 960Âcmâ^'1 FTIR peak. Microporous and Mesoporous Materials, 2015, 210, 69-76.	4.4	66
67	Direct Aqueous-Phase Synthesis of Sub-10 nm "Luminous Pearls―with Enhanced <i>in Vivo</i> Renewable Near-Infrared Persistent Luminescence. Journal of the American Chemical Society, 2015, 137, 5304-5307.	13.7	357
68	Achieving Low Overpotential Li–O <sub>2</sub> Battery Operations by Li <sub>2</sub> O <sub>2</sub> Decomposition through One-Electron Processes. Nano Letters, 2015, 15, 8371-8376.	9.1	70
69	Direct, single-step synthesis of hierarchical zeolites without secondary templating. Journal of Materials Chemistry A, 2015, 3, 1298-1305.	10.3	66
70	Efficient mechano-catalytic depolymerization of crystalline cellulose by formation of branched glucan chains. Green Chemistry, 2015, 17, 769-775.	9.0	58
71	Dehydration of fructose into furans over zeolite catalyst using carbon black as adsorbent. Microporous and Mesoporous Materials, 2014, 191, 10-17.	4.4	70
72	Textural and catalytic properties of Mo loaded hierarchical meso-/microporous lamellar MFI and MWW zeolites for direct methane conversion. Applied Catalysis A: General, 2014, 470, 344-354.	4.3	44

#	Article	IF	CITATIONS
73	Base free, one-pot synthesis of lactic acid from glycerol using a bifunctional Pt/Sn-MFI catalyst. Green Chemistry, 2014, 16, 3428-3433.	9.0	100
74	Template-Free Ordered Mesoporous Silicas by Binary Nanoparticle Assembly. Langmuir, 2014, 30, 11802-11811.	3.5	18
75	Effective C–O Bond Cleavage of Lignin β-O-4 Model Compounds: A New RuHCl(CO)(PPh3)3/KOH Catalytic System. Catalysis Letters, 2014, 144, 1159-1163.	2.6	30
76	Photocatalytic degradation of 17α-ethinylestradiol (EE2) in the presence of TiO2-doped zeolite. Journal of Hazardous Materials, 2014, 279, 17-25.	12.4	80
77	On Asymmetric Surface Barriers in MFI Zeolites Revealed by Frequency Response. Journal of Physical Chemistry C, 2014, 118, 22166-22180.	3.1	47
78	On the kinetics of the isomerization of glucose to fructose using Sn-Beta. Chemical Engineering Science, 2014, 116, 235-242.	3.8	57
79	Dual Template Synthesis of Meso- and Microporous MFI Zeolite Nanosheet Assemblies with Tailored Activity in Catalytic Reactions. Chemistry of Materials, 2014, 26, 1345-1355.	6.7	119
80	Synthesis of Hierarchical Sn-MFI as Lewis Acid Catalysts for Isomerization of Cellulosic Sugars. ACS Catalysis, 2014, 4, 2029-2037.	11.2	108
81	Ultra-selective cycloaddition of dimethylfuran for renewable p-xylene with H-BEA. Green Chemistry, 2014, 16, 585-588.	9.0	220
82	Promoting Interspecies Electron Transfer with Biochar. Scientific Reports, 2014, 4, 5019.	3.3	429
83	Enhanced Molecular Transport in Hierarchical Silicalite-1. Langmuir, 2013, 29, 13943-13950.	3.5	56
84	Confined synthesis of three-dimensionally ordered mesoporous-imprinted zeolites with tunable morphology and Si/Al ratio. Microporous and Mesoporous Materials, 2013, 181, 8-16.	4.4	50
85	Reactive adsorption for the selective dehydration of sugars to furans: Modeling and experiments. AICHE Journal, 2013, 59, 3378-3390.	3.6	32
86	Engineering the Upconversion Nanoparticle Excitation Wavelength: Cascade Sensitization of Triâ€doped Upconversion Colloidal Nanoparticles at 800 nm. Advanced Optical Materials, 2013, 1, 644-650.	7.3	321
87	A novel method for the preparation of Ru(bpy)32+-doped silica nanoparticles. Materials Letters, 2013, 92, 17-20.	2.6	6
88	Dominance of Surface Barriers in Molecular Transport through Silicalite-1. Journal of Physical Chemistry C, 2013, 117, 25545-25555.	3.1	86
89	Production of <i>p</i> â€Xylene from Biomass by Catalytic Fast Pyrolysis Using ZSMâ€5 Catalysts with Reduced Pore Openings. Angewandte Chemie - International Edition, 2012, 51, 11097-11100.	13.8	199
90	Characterization of the Pore Structure of Three-Dimensionally Ordered Mesoporous Carbons Using High Resolution Gas Sorption. Langmuir, 2012, 28, 12647-12654.	3.5	85

#	Article	IF	CITATIONS
91	Rapid synthesis of Sn-Beta for the isomerization of cellulosic sugars. RSC Advances, 2012, 2, 10475.	3.6	107
92	Cycloaddition of Biomass-Derived Furans for Catalytic Production of Renewable <i>p</i> -Xylene. ACS Catalysis, 2012, 2, 935-939.	11.2	400
93	Production of Renewable Aromatic Compounds by Catalytic Fast Pyrolysis of Lignocellulosic Biomass with Bifunctional Ga/ZSMâ€5 Catalysts. Angewandte Chemie - International Edition, 2012, 51, 1387-1390.	13.8	338
94	Sub-40 nm Zeolite Suspensions via Disassembly of Three-Dimensionally Ordered Mesoporous-Imprinted Silicalite-1. Journal of the American Chemical Society, 2011, 133, 493-502.	13.7	91
95	Hydrothermal Synthesis of Zeolites with Three-Dimensionally Ordered Mesoporous-Imprinted Structure. Journal of the American Chemical Society, 2011, 133, 12390-12393.	13.7	266
96	Ethanol Dehydration to Ethylene in a Stratified Autothermal Millisecond Reactor. ChemSusChem, 2011, 4, 1151-1156.	6.8	19
97	Silicaâ€Nanoparticle Coatings by Adsorption from Lysine–Silicaâ€Nanoparticle Sols on Inorganic and Biological Surfaces. Angewandte Chemie - International Edition, 2011, 50, 1617-1621.	13.8	28
98	A New, Yet Familiar, Lamellar Zeolite. ChemCatChem, 2010, 2, 246-248.	3.7	14
99	Hollow cubic silica shells and assembled porous coatings. Scripta Materialia, 2010, 62, 504-507.	5.2	2
100	Self-Assembly of Fibronectin Mimetic Peptide-Amphiphile Nanofibers. Langmuir, 2010, 26, 1953-1959.	3.5	76
101	Binding of the Fibronectin-Mimetic Peptide, PR_b, to α <sub>5</sub> 1² <sub>1</sub> on Pig Islet Cells Increases Fibronectin Production and Facilitates Internalization of PR_b Functionalized Liposomes. Langmuir, 2010, 26, 14081-14088.	3.5	23
102	One-Dimensional Assembly of Silica Nanospheres Mediated by Block Copolymer in Liquid Phase. Journal of the American Chemical Society, 2009, 131, 16344-16345.	13.7	46
103	Mechanism of Formation of Uniform-Sized Silica Nanospheres Catalyzed by Basic Amino Acids. Chemistry of Materials, 2009, 21, 3719-3729.	6.7	169
104	Changes in the medium-range order during crystallization of aluminosilicate zeolites characterized by high-energy X-ray diffraction technique. Journal of the Ceramic Society of Japan, 2009, 117, 277-282.	1.1	20
105	Microwave-induced synthesis of highly dispersed gold nanoparticles within the pore channels of mesoporous silica. Journal of Solid State Chemistry, 2008, 181, 957-963.	2.9	40
106	Nanoscale Reactor Engineering: Hydrothermal Synthesis of Uniform Zeolite Particles in Massively Parallel Reaction Chambers. Angewandte Chemie - International Edition, 2008, 47, 9096-9099.	13.8	36
107	Inside Cover: Nanoscale Reactor Engineering: Hydrothermal Synthesis of Uniform Zeolite Particles in Massively Parallel Reaction Chambers (Angew. Chem. Int. Ed. 47/2008). Angewandte Chemie - International Edition, 2008, 47, 8970-8970.	13.8	0
108	Innentitelbild: Nanoscale Reactor Engineering: Hydrothermal Synthesis of Uniform Zeolite Particles in Massively Parallel Reaction Chambers (Angew. Chem. 47/2008). Angewandte Chemie, 2008, 120, 9106-9106.	2.0	0

#	Article	IF	CITATIONS
109	Hierarchical nanofabricationÂofÂmicroporous crystals with ordered mesoporosity. Nature Materials, 2008, 7, 984-991.	27.5	553
110	Synthesis of Nanometer-Sized Sodalite Without Adding Organic Additives. Langmuir, 2008, 24, 6952-6958.	3.5	66
111	Intermediate-range Order in Mesoporous Silicas Investigated by a High-energy X-ray Diffraction Technique. Chemistry Letters, 2008, 37, 30-31.	1.3	10
112	Role of heteroatoms in precursor formation of zeolites. Studies in Surface Science and Catalysis, 2007, 170, 506-511.	1.5	2
113	New insights into the formation of microporous materials by in situ scattering techniques. Faraday Discussions, 2007, 136, 157.	3.2	34
114	In situ Small-Angle and Wide-Angle X-ray Scattering Investigation on Nucleation and Crystal Growth of Nanosized Zeolite A. Chemistry of Materials, 2007, 19, 1906-1917.	6.7	87
115	Effects of silicon sources on the formation of nanosized LTA: An in situ small angle X-ray scattering and wide angle X-ray scattering study. Microporous and Mesoporous Materials, 2007, 101, 134-141.	4.4	22
116	Crystal structures and spectroscopic properties of a new zinc phosphite cluster and an unexpected chainlike zinc phosphate obtained by hydrothermal reactions. Journal of Solid State Chemistry, 2007, 180, 981-987.	2.9	8
117	Organic–Inorganic Mesoporous Nanocarriers Integrated with Biogenic Ligands. Small, 2007, 3, 1740-1744.	10.0	114
118	Synthesis of a Three-Dimensional Cubic Mesoporous Silica Monolith Employing an Organic Additive through an Evaporation-Induced Self-Assembly Process. Langmuir, 2006, 22, 6391-6397.	3.5	23
119	Versatile Fabrication of Distorted Cubic Mesoporous Silica Film Using CTAB Together with a Hydrophobic Organic Additive. Journal of Physical Chemistry B, 2006, 110, 9751-9754.	2.6	16
120	A new approach to the determination of atomic-architecture of amorphous zeolite precursors by high-energy X-ray diffraction technique. Physical Chemistry Chemical Physics, 2006, 8, 224-227.	2.8	88
121	In situ observation of homogeneous nucleation of nanosized zeolite A. Physical Chemistry Chemical Physics, 2006, 8, 1335.	2.8	32
122	A New Organically Templated Zinc Phosphite Synthesized in Phosphorous Acid Flux and Its Hydrothermal Analogue. Crystal Growth and Design, 2006, 6, 2435-2437.	3.0	22
123	Synthesis and Characterization of a New Three-dimensional Organically Templated Nickel-Zinc Phosphate. Zeitschrift Fur Anorganische Und Allgemeine Chemie, 2006, 632, 465-468.	1.2	2
124	A novel layered bimetallic phosphite intercalating with organic amines: Synthesis and characterization of Co(H2O)4Zn4(HPO3)6·C2N2H10. Journal of Solid State Chemistry, 2006, 179, 723-728.	2.9	18
125	Phase selection of FAU and LTA zeolites by controlling synthesis parameters. Microporous and Mesoporous Materials, 2006, 89, 227-234.	4.4	60
126	Phase transformation in mesoporous silica films induced by the degradation of organic moiety. Journal of Porous Materials, 2006, 13, 303-306.	2.6	2

#	Article	IF	CITATIONS
127	[Ge9O14(OH)12](C6N2H16)22H2O: A Novel Germanate with Ge?O Helical Chains Formed by Hydrothermal Synthesis that Can Separatetrans andcis Isomers in Situ. European Journal of Inorganic Chemistry, 2004, 2004, 4547-4549.	2.0	9
128	The Hydrothermal Synthesis and Crystal Structure of (H2O)[Ge5O10] and [(CH3)4N][Ge10O20OH], Two Novel Porous Germanates ChemInform, 2004, 35, no.	0.0	0
129	The Hydrothermal Synthesis and Crystal Structure of (H2O)[Ge5O10] and [(CH3)4N][Ge10O20OH], Two Novel Porous Germanates. Chemistry Letters, 2004, 33, 74-75.	1.3	17
130	Improving Yields and Catalyst Reuse for Palmitic Acid Aromatization in the Presence of Pressurized Water. ACS Sustainable Chemistry and Engineering, 0, , .	6.7	1